



NLR-TP-2003-557

Accident risk assessment of simultaneous converging instrument approaches

H.A.P. Blom, M.B. Klompstra and G.J. Bakker



NLR-TP-2003-557

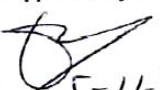
Accident risk assessment of simultaneous converging instrument approaches

H.A.P. Blom, M.B. Klompstra and G.J. Bakker

This report is based on a paper published in Air Traffic Control Quarterly, Vol 11 (2), pp. 123-155, 2003. Parts of this research have been performed with support of CAA and the ATC The Netherlands.

The contents of this report may be cited on condition that full credit is given to NLR and the authors.

Customer: National Aerospace Laboratory NLR
Working Plan number:
Owner: National Aerospace Laboratory NLR
Division: Air Transport
Distribution: Unlimited
Classification title: Unclassified
October 2003

Approved by author:  5-11-'03	Approved by project manager:  11-11-'03	Approved by project managing department:  11-11-'03
--	--	--



ACCIDENT RISK ASSESSMENT OF SIMULTANEOUS CONVERGING INSTRUMENT APPROACHES

Henk A.P. Blom, Margriet B. Klompstra and Bert Bakker

ABSTRACT

With increasing traffic there often are environmental and economical reasons to optimise Simultaneous Converging Instrument Approaches (SCIA) without sacrificing the high safety levels realised in air traffic. One of the well known safety issues of SCIA is the risk of a mid air collision due to a double missed approach. The aim of this paper is to show through a working example that there is a clear advantage to evaluate the safety through support of advanced accident risk assessment methodology. In this paper such methodology is applied to a specific example of SCIA at Amsterdam Airport Schiphol. Comparison of the obtained results against FAA established SCIA criteria shows that there are situations in which these FAA criteria are not met; however, the collision risk is not higher than for similar situations that would satisfy these criteria. The implication for Amsterdam Airport Schiphol is that a specific change can be introduced as being risk neutral. The implication for other busy airports with converging runways might be that there is room to develop new or improved SCIA without compromising safety.



Contents

1	Introduction	5
1.1	Existing SCIA criteria	5
1.2	Example considered	6
1.3	Phase 1 study	7
1.4	Phase 2 study	7
1.5	Aim and organisation of this paper	8
2	Modelling of missed approaches	9
2.1	Landing traffic flows	9
2.2	Missed approach frequencies	9
2.3	Missed approach initiation heights	12
2.4	Missed approach climb behaviour	13
2.5	Turn during missed approach	14
2.6	Controller turn instructions	15
3	Mathematical modelling	17
3.1	Integration of mathematical models	17
3.2	Risk of collision between aircraft	19
3.3	Collision risk per approach	20
3.4	Aircraft types and double missed approach causes	21
3.5	Decomposition over manoeuvre combinations	21
3.6	Decomposition of incrossing rate	22
3.7	Numerical evaluation of equations	23
4	Risk assessment of operational scenarios	24
4.1	Operational scenarios	24
4.2	Model based conditional collision risk	25
4.3	Model based collision risk	25
4.4	Bias and uncertainty assessment	27
4.5	Comparison against risk criteria	29
5	Conclusions	32
5.1	Conclusions regarding SCIA on 19R×22	32
5.2	General conclusions regarding SCIA	33
6	References	35
	Acronyms and abbreviations	37
	Symbols	38

(40 pages in total)



1 Introduction

Many airports in the world have converging runways. Due to increasing traffic, these airports have environmental and economic incentives to allow for Simultaneous Converging Instrument Approaches (SCIA) without compromising established safety levels. And if safe SCIA were not feasible, then Dependent Converging Instrument Approaches (DCIA) are another option. One of the well known safety issues of SCIA and DCIA is to safely manage a double missed approach (MA). The basic studies on these safety management issues have been performed by MITRE; first for SCIA [Newman et al., 1981; Weiss, 1986], and later for DCIA [Smith et al., 1992]. The analysis used in these basic studies consists of a systematic “worst” case reasoning about MAs. This might lead to safety conservative requirements on SCIA and on DCIA. The aim of the current paper is to show through an example that the existing criteria of allowing SCIA indeed may be relaxed by systematically exploiting an accident risk assessment modelling approach.

1.1 Existing SCIA criteria

Although ICAO provides criteria for simultaneous instrument operations on parallel or near parallel runways [ICAO, 1988], these criteria do not address SCIA. The FAA, however, has systematically developed SCIA criteria [FAA, 1993], which are often referred to as the TERPS+3 criteria, and which come down to:

1. Non-intersecting straight-in final approach courses;
2. MA Points (MAPt's), for latest yes/no landing decision, must be at least 3 nautical miles apart;
3. Published MA paths diverge by at least 45 degrees and the associated primary TERPS surfaces do not overlap;
4. ATC shall designate separation responsibility and procedures to be applied in the event of a MA initiated beyond the MAPt;
5. ATC may establish higher weather minima than published to preclude, to the extent feasible, the possibility of a weather related MA.

By McCartor et al. [1997], it has also been shown that properly equipped FMS aircraft that execute a MA on the autopilot could do much better than criterion 3 requires. In line with this, for a limited category of aircraft, criterion 3 has been tightened and criterion 2 has been replaced by the requirement that the MAPt on the secondary runway should not be lower than 650 feet [FAA, 1998].

For airports that frequently experience low ceiling conditions, the FAA criteria imply a serious limitation in the effective exploitation of SCIA, and a similarly frequent limitation of airport



capacity. Hence from an airport capacity point of view it would be very valuable to have an approach that allows relaxation of the existing SCIA criteria, 2 and 3 in particular.

1.2 Example considered

The specific example considered in this paper is SCIA on runways 19R and 22 of Amsterdam Airport Schiphol, the geometry of which is depicted in Figure 1. As explained below, for this example TERPS+3 criteria 1, 2, 4 and 5 are satisfied, and 3 is not.

Runway 19R is one of Schiphol's four main runways. It has its MAPt at 0.46 nautical miles before the threshold (ILS height is 200 ft) and has a straight MA path, while runway 22 is a secondary non-intersecting runway with its MAPt at 1 nautical mile before the threshold (ILS height is 350 feet) and a MA path that is 63 degrees turning left [AIP, 2000]. The distance between the two MAPt's is 3.03 nmi; hence the first and second TERPS+3 criteria of [FAA, 1993] are satisfied. Since the MA paths diverge by 25° only, which is less than the required 45°, the third TERPS+3 criterion is not satisfied. The 19R runway controller is prepared to instruct a right turning MA to an aircraft on 19R if an aircraft on 22 makes a straight MA, which means that the 4th TERPS+3 criterion is satisfied. Finally, allowance of SCIA on runways 19R and 22 is limited to conditions of relatively high headwind for runway 22, i.e. this falls within the 5th TERPS+3 criterion.

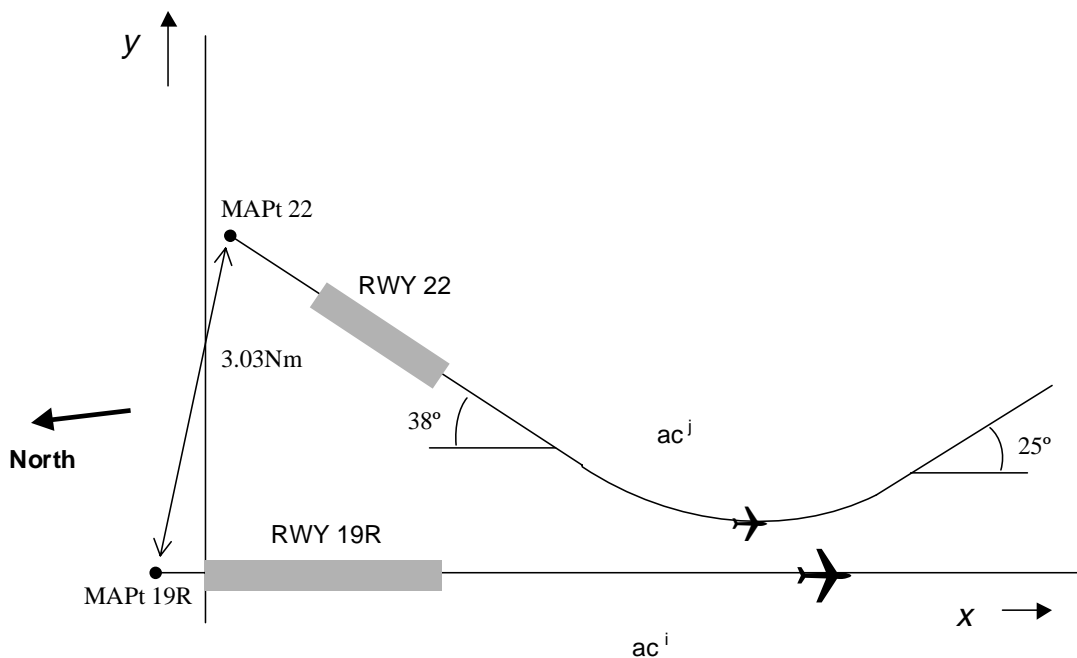


Figure 1 Geometry of runways 19R and 22 at Amsterdam Airport Schiphol and the AIP specified missed approach paths.



When runway 22 is in use the lowest forecasted broken-clouds-ceiling for selecting runway 22 as landing runway is 400ft. Frequent low broken-clouds-ceiling conditions at Amsterdam Airport Schiphol invite a lowering of this selection criterion to 300 ft, and to do so the MAPt for runway 22 should be shifted some 0.5 nmi towards the threshold. Then the distance between the MAPt's of runway 22 and 19R would become 2.86 nmi, which would mean that TERPS+3 criterion number 2 is no longer satisfied for SCIA on runways 22 and 19R. In order to determine whether there exists a sound rationale for applying risk criteria numbers 2 and 3 to this example, a risk assessment modelling study has been conducted following the approach of [Blom et al., 2001a]. This modelling study is organised in two phases:

- Phase 1: to develop an initial risk assessment model that is able to make a relative comparison of accident risks due to double MAs with the old and the new MAPt's.
- Phase 2: to refine the risk assessment model such that it enables a comparison of the risk due to double MAs with established accident risk criteria for en-route traffic.

1.3 Phase 1 study

During phase 1, relative accident risk assessments have been performed for two situations: one with the MAPt for runway 22 at 1 nmi before the threshold, and the other with the MAPt shifted 0.5 nmi towards the threshold. As a result of this shift, the distance between the MAPt's reduces from 3.03 nmi to 2.86 nmi, the latter of which is below the 3 nmi of the 2nd TERPS+3 criterion. The steps performed are:

- Identification of existing and new operations, including the relevant scenarios and the associated hazards, both through brainstorming and interviews with experts, and through making use of dedicated hazard and incident data bases.
- Development of the mathematical model, including model assumptions and assessment of parameter values, and integration with the identified scenarios.

The key finding of phase 1 was that the developed model of the SCIA operation on 19R and 22 is risk neutral with respect to the proposed shifting of the MAPt for runway 22 towards its threshold [Blom et al., 2001b]. The rationale for this finding is that in the model the largest contribution to accident risk stems from a non-negligible probability that both aircraft follow a straight MA path. This finding also implied that it would not improve safety to increase the MA path turning angle for runway 22 such that the 3rd TERPS+3 criterion would be satisfied.

1.4 Phase 2 study

The aim of the phase 2 study is to refine the risk assessment model and subsequently compare the double MA's risk of conducting SCIA on runways 19R×22 against established collision risk criteria. The steps performed are:



- In order to allow for a significant reduction of the level of uncertainty in the assessed risk, site-specific statistical data on MAs and their reasons has been collected in collaboration with ATC the Netherlands.
- On the basis of this information, the accident risk assessment model and its assumptions were further improved, and subsequently the modelled accident risk was evaluated.
- Subsequently, a bias and uncertainty analysis was performed, following a recently developed approach [Everdij and Blom, 2002].
- Finally, the obtained accident risk results were compared against a risk criterion that is derived from ICAO's TLS for collision between en-route flying aircraft [ICAO, 1998].

1.5 Aim and organisation of this paper

This paper aims to present the phase 2 results and is organised as follows. First, an overview is provided of the main probabilistic models collected during both phases for the Schiphol example considered. Then an explanation shows how these probabilistic models are integrated into a mathematical collision risk model. This is followed by a section that introduces the specific Schiphol example scenarios that have been evaluated during phase 2, and gives the accident risk results obtained for these scenarios. Finally a summary of findings and conclusions is given both for the specific Schiphol example and for the TERPS+3 criteria for SCIA in general.



2 Modelling of missed approaches

One of the important steps required for the accident risk assessment is to develop probabilistic models of MAs. The aim of this section is to explain the main issues covered by this modelling:

- Landing traffic flows
- MA frequencies
- MA initiation height
- MA climb behaviour
- Turn during MA
- Controller turn instruction

In addition to this, other probabilistic models have been adopted for issues such as aircraft speed behaviour, wind conditions, and the size of the aircraft involved. Details are given in [Blom et al., 2001d].

2.1 Landing traffic flows

Based on the evaluation of statistical data for the percentages of landing heavy/medium/light aircraft on runways 19R and 22, the following percentages of arrival weight category, as shown in Table 1, have been chosen for 19R and 22. This is referred to as **Model assumption M.1**. The arrival spread over the weight classes is based on arrival trajectories reconstructed from radar data over several one-month periods. This has shown that the uncertainty of assumption **M.1** is small.

	Arrivals on 19R	Arrivals on 22
Heavy	22%	0%
Medium	78%	85%
Light	0%	15%

Table 1 Arrival category percentages.

The traffic flow is assumed to be 30 arrivals per hour for each runway. This is referred to as **Model assumption M.37**. Furthermore it is assumed that none of this traffic is equipped with TCAS, and that no use is made of see-and-avoid. This is covered by **Model assumptions M.15** and **M.16** respectively.

2.2 Missed approach frequencies

During the first phase of the study there appeared to be significant uncertainty regarding the frequencies of MAs [Blom et al., 2001b]. During the second phase of the study this problem has been addressed through making use of the fact that since June 1995 tower controllers at Schiphol have systematically been reporting MAs as part of the safety management process of



ATC the Netherlands. This data set covering June 1995 through mid December 2000 has been analysed in a statistical sense. The first analysis was directed towards the variety in reasons and the percentages, the result of which is depicted in Table 2 for both uncommon and potentially common causes.

Further analysis of the MA reports has shown that there were 21 reported double (or triple) MAs within 4 minutes, from which 15 are subsequent MAs of aircraft that were approaching the same runway under proper separation conditions. This leaves 6 double or triple MAs on converging runways (all within 2 minutes):

- One coincidentally double MA (shorthand notation: Coinc)¹,
- One double MA caused by Tower R/T down (shorthand notation: Tower),
- One triple MA and one double MA caused by severe Wind (shorthand notation: Wind),
- One triple MA caused by Meteo info down (shorthand notation: Meteo),
- One double MA caused by severe wind during Mixed mode operation, i.e. a departure in between arrivals. In this case, severe wind initiated a MA for an arrival at one runway. In response to this a departure aircraft on the other runway had to wait, and the subsequent arrival aircraft on the same runway had to initiate a MA too (shorthand notation: Mixed).

It was also verified if any of these double or triple MAs had led to a critical incident; it turned out that none of them had done so.

Besides the above mentioned causes for a double MA, also airport great Alert (i.e. closing the airport e.g. because of a major fire) has been identified as a cause for a double MA (shorthand notation: Alert).

On the basis of these statistical MA data, expert based estimates of relevant exposure frequencies and MA reporting reliability, double MA frequencies have been estimated, they are given in Table 3 and referred to as **Model Assumption M.30a**. Table 3 also gives the equations that are used for this evaluation. $\hat{N}_{\text{Single}} = 10^6$ is the estimated number of landings at Schiphol over the period considered, $\hat{n}_{\text{Single}} = 1240$, $\hat{n}_{\text{Tower}} = 2$, $\hat{n}_{\text{Wind}} = 3.5$, $\hat{n}_{\text{Meteo}} = 2.5$, $\hat{n}_{\text{Alert}} = 1$ and $\hat{n}_{\text{Mixed}} = 2$ are obtained as Bayesian estimates from the single, double and triple MA counts, and $\hat{v}_{\text{Simult}} = 0.4$ and $\hat{v}_{\text{MixedSimult}} = 0.025$ are expert based exposure frequency estimates. The last value shows that, during simultaneous landings, mixed mode operations were conducted in exceptional cases only at Amsterdam Airport Schiphol.

¹ Shorthand notation is used in mathematical symbols.



Reason	Percentage
UNCOMMON CAUSES	59.8 %
Crew related	4.2 %
Misunderstood R/T	0.7 %
Wrong R/T frequency	1.3 %
Wrong approach charts	0.3 %
Cabin not ready	1.5 %
Unintended MA	0.5 %
Technical aircraft	25.5 %
Bird strike	0.9 %
Technical unknown	2.2 %
Technical various	1.1 %
Gear (door) problems	14.2 %
Flap problems	5.8 %
Autopilot / nav receiver	1.2 %
Unstable approach/landing	24.9 %
ILS failed	0.4 %
Wake turbulence	1.1 %
Unstable approach	5.7 %
Speed high	1.7 %
Altitude high	13.5 %
Ground Proximity Warning System alerts	2.6 %
Separation reasons	4.1 %
Lateral separation	3.8 %
TCAS	0.3%
Unknown	1.1%
Unknown	1.1 %
POTENTIALLY COMMON CAUSE	40.2 %
Late/no landing clearance	21.2 %
Blocked R/T, ATCo busy	2.6 %
Landing runway occupied by aircraft	16.6 %
Landing runway occupied by other	2.0 %
Weather	19.0 %
Visibility / Runway Visual Range / cloud	5.0 %
Wind (gust)	5.5 %
Wind shear	6.9 %
Lightning / showers	1.6 %
TOTAL	100%

Table 2 Percentages of controller reported reasons for initiation of a MA at Amsterdam Airport Schiphol.



Single MA	$\hat{\rho}_{\text{Single}} = \frac{\hat{n}_{\text{Single}}}{\hat{N}_{\text{Single}}}$	$1.24 \cdot 10^{-3}$
Coincidentally double MA	$\hat{\rho}_{\text{Coinc}} = (\hat{\rho}_{\text{Single}})^2$	$0.15 \cdot 10^{-5}$
Double MA and Tower R/T blocked	$\hat{\rho}_{\text{Tower}} = \frac{\hat{n}_{\text{Tower}}}{\frac{1}{2} \hat{N}_{\text{Single}} \cdot \hat{v}_{\text{Simult}}}$	$1.0 \cdot 10^{-5}$
Double MA and severe Wind	$\hat{\rho}_{\text{Wind}} = \frac{\hat{n}_{\text{Wind}}}{\frac{1}{2} \hat{N}_{\text{Single}} \cdot \hat{v}_{\text{Simult}}}$	$1.75 \cdot 10^{-5}$
Double MA and Meteo info down	$\hat{\rho}_{\text{Meteo}} = \frac{\hat{n}_{\text{Meteo}}}{\frac{1}{2} \hat{N}_{\text{Single}} \cdot \hat{v}_{\text{Simult}}}$	$1.25 \cdot 10^{-5}$
Double MA and great Alert	$\hat{\rho}_{\text{Alert}} = \frac{\hat{n}_{\text{Alert}}}{\frac{1}{2} \hat{N}_{\text{Single}} \cdot \hat{v}_{\text{Simult}}}$	$0.5 \cdot 10^{-5}$
Double MA and Mixed mode operation	$\hat{\rho}_{\text{Mixed}} = \frac{\hat{n}_{\text{Mixed}}}{\frac{1}{2} \hat{N}_{\text{Single}} \cdot \hat{v}_{\text{Simult}} \cdot \hat{v}_{\text{Mixed Simult}}}$	$4.0 \cdot 10^{-4}$

Table 3 Estimated MA frequencies and the equations used.

Due to the use of a Bayesian estimation approach a zero count leads to a non zero expectation and the uncertainty in the estimated frequency values is also known. For all except mixed mode, the 95% uncertainty interval for the frequency values goes a factor 1.5 up and a factor 1.5 down. For mixed mode, this uncertainty interval is a factor $(1.5)^2$.

2.3 Missed approach initiation heights

Since the MA initiation heights in the Schiphol data set either were often not reported or not well reported, use has been made of world-wide KLM pilot MA reports over the time period September 1992 to May 1994 [Blom et al., 2001d]. This data provides an indication for the reasons of initiating MAs, and their altitude and frequency of occurrence. Based on this data, a histogram has been constructed of MA initiation heights. Subsequently, this histogram has been fitted with a weighted sum of a Rayleigh density and a uniform density as depicted in Figure 2. The probability density function of MA initiation height is a density fit of this histogram, which is a weighted sum of Rayleigh density (60%) with mean 300ft and a Uniform density (40%). This is referred to as **Model assumption M.4**.

It is also assumed that for each of the double MA causes in Table 3 only one of the following two densities applies:

- The Rayleigh density for double MAs initiated due to Tower R/T blocked and due to severe Wind.



- The uniform density for all other double MAs.

Since the histogram is based on the world-wide trip reports of one airline, there may be a significant uncertainty level in the shape of the histogram, and thus in the fitted densities (60% Rayleigh and 40% Uniform).

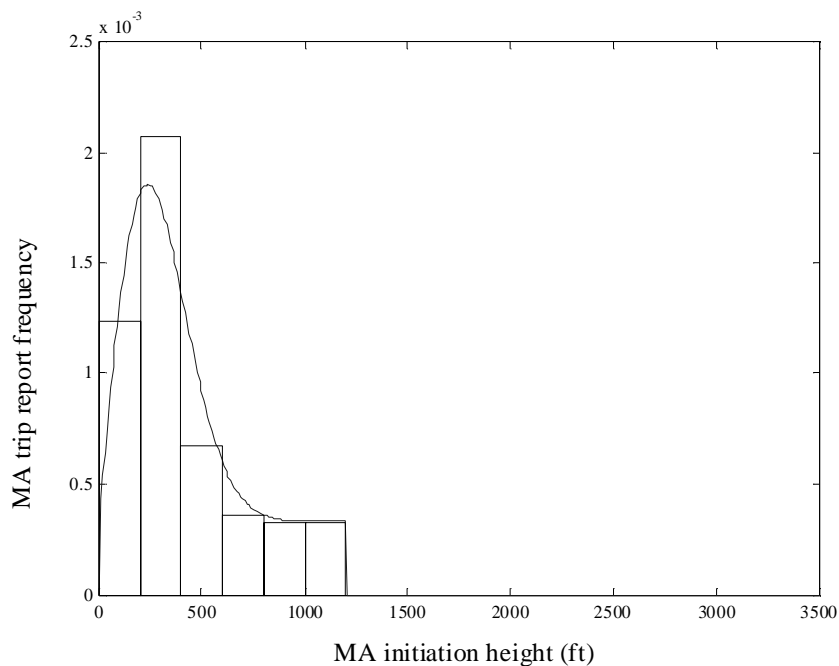


Figure 2 Histogram of KLM pilot MA trip reports and of density fit, which is a weighted sum of a Rayleigh density (60%) with mean 300ft and a Uniform density on 0-1200ft (40%).

2.4 Missed approach climb behaviour

Based on [ICAO-CRM, 1980], probabilistic models for the lateral deviations from nominal MA paths are available; this is referred to as **Model assumption M.6a**. For vertical behaviour during MA, ICAO-CRM provides a parabolic vertical path model for the change from descent to climb, and then a model for minimum climb rate requirement only (2.5%). The parabolic vertical path model has been adopted as **Model assumption M.6c**, and the minimal climb rate requirement is used for 1% of the MA climbs to cover non-nominal climbs.

McCortor et al. [1997] provides histograms of simulated FMS-LNAV climb performance during MAs. As a reasonable approximation of these densities, we assumed a Gaussian density with mean value 10 m/s and standard deviation of 2 m/s for the other 99% MAs. This particular combination of models is referred to as **Model assumption M.5**.



The rate of climb is assumed to continue until the final MA altitude (of 2000ft) has been reached; this is referred to as **Model assumption M.18**. In reality aircraft level off gradually on autopilot, or may overshoot when levelling off without autopilot.

Once the final MA altitude has been reached it is assumed that for all aircraft weight categories (heavy, medium and light), the vertical deviations at final MA altitude are assumed to be Gaussian with standard deviation of 10 m. This is referred to as **Model assumption M.6b**. The true standard deviation may be up to a factor 2 larger or smaller, and thus there is a significant uncertainty².

2.5 Turn during missed approach

Although in most cases a turn is made when it is prescribed by the AIP, there is a non-zero probability α_{AIP} that a pilot forgets to make a turn during the MA as prescribed in the AIP. Assuming that the pilots are well aware of the AIP published MA path, (**Model assumption M.11**), the expert-based estimated values for α_{AIP} vary from 0.05 to 0.22, with 0.10 as best estimate. The last value is referred to as **Model assumption M.29**.

Based on information collected from experienced (airline) pilots on various aircraft, it was identified that the logical moment at which the pilot starts a turn during a MA is where the pilot completes a well trained sequence of aircraft reconfiguration activities and the aircraft has reached sufficient height. This expert knowledge has resulted in the development of probabilistic models for the reconfiguration of an aircraft during MA, which are referred to as **Model assumption M.20**, and the details of which are given for Boeing 737 and Airbus A320 in Table 4. A similar model has been identified for Boeing 767/300, Boeing 747, Fokker 50, Cessna 172 and Swearingen Metro II [See Blom et al, 2001d].

In addition, Boeing 747 and 767/300 are assumed to be representative for the heavy category aircraft, Boeing 737 and Airbus A320 are assumed to be representative for 50% of the medium category aircraft, while the Fokker 50 is assumed to be representative for the other 50% of the medium category aircraft. Swearingen Metro II and Cessna 172 are each assumed to be representative for 50% of the light category aircraft.

² At North Atlantic en-route levels the vertical deviation has a standard deviation of 24.9 m [ICAO-RGSCP, 1988, pp 1A-149] and according to experts this deviation is lower at the final MA altitude.



Task	Starts at	Duration		Ends at
		50%	95%	
1	T1 (= MA initiation point)	1 s	3 s	T2
2	T2	6 s	9 s	T3
3	T1 + 1 second	4 s	8 s	T4
4	T1 + 2 seconds	6 s	10 s	T5
5	T4	3 s	10 s	T6
6	T6 & passed 1000 ft	1300 ft	1600 ft	T7
7	T6 & passed 400 ft	600 ft	900 ft	T8
8	Passed altitude of 2000 ft – (10% of climb rate in fpm)	1700 ft	1900 ft	T9

Table 4 Boeing 737 / Airbus A320 MA task breakdown. The tasks are: 1) Triggering MA flight director mode, 2) Thrust change to MA thrust, 3) Adjusting pitch angle, 4) Raising flaps to climb-out setting, 5) Raising the gear, 6) Engaging the autopilot, 7) Turn. Adjusting lateral navigation, 8) Level off, Adjusting vertical navigation.

2.6 Controller turn instructions

If aircraft on runways 22 and 19R both make a MA then the way of working is that the 19R runway controller issues a preventive right turn instruction to the aircraft on 19R. It is assumed that the controllers of runways 19R and 22 monitor aircraft well on initiating a MA and inform each other immediately of such event. This is referred to as **Model assumption M.10**. It is assumed that the controller of runway 22 does not issue a manoeuvre instruction (**Model assumption M.31**). Subsequently the instruction by the 19R controller should reach the pilots of aircraft on 19R. The chances to accomplish this vary significantly with the double MA causing conditions. Expert estimates for the probability that a 19R controller is not successful in letting the pilot on 19R make a right turn in case of a double MA are provided in Table 5. The expected values are referred to as **Model assumption M.30b**.

Symbol	Expected	Max	Min
α_{Coinc}	0.15	0.30	0.05
α_{Tower}	0.50	0.99	0.25
α_{Wind}	0.15	0.30	0.05
α_{Meteo}	0.05	0.10	0.02
α_{Alert}	0.05	0.10	0.02
α_{Mixed}	0.05	0.10	0.02

Table 5 Expert estimated values for the probability that the 19R controller is not successful in letting the aircraft on 19R make a right turn in case of a double MA.



A properly received ATCo turn instruction is assumed to be implemented by the pilot immediately upon completion of the reconfiguration activities. This is referred to as **Model assumption M.12**. It is also assumed that this reception of such instruction from the controller does not lead to any delay in the completion of the reconfiguration tasks (**Model assumption M.13**).

In order to validate **M.12**, **M.13** and **M.20** to a reasonable extent, KLM has performed Boeing 737 flight simulator sessions with 21 different flight crews, in which a sudden runway non-availability was simulated. Subsequently, during the late initiated MA a pseudo controller suddenly issued a turn instruction. The observed moments of starting a turn agreed quite well with the probabilistic model. It also became clear that during these simulator sessions, sharper turns were realised than assumed in the model. In addition to this, Expert Judgement Interviews have been held with five experienced TWR/APP Air Traffic Controllers.

3 Mathematical modelling

3.1 Integration of mathematical models

For the integration of the mathematical models, the Dynamically Coloured Petri Net (DCPN) approach is used [Everdij et al., 1997; Everdij and Blom, 2000]. During DCPN development, use is made of a functional representation of ATM. The functional subsystems and their interrelations are depicted in Figure 3.

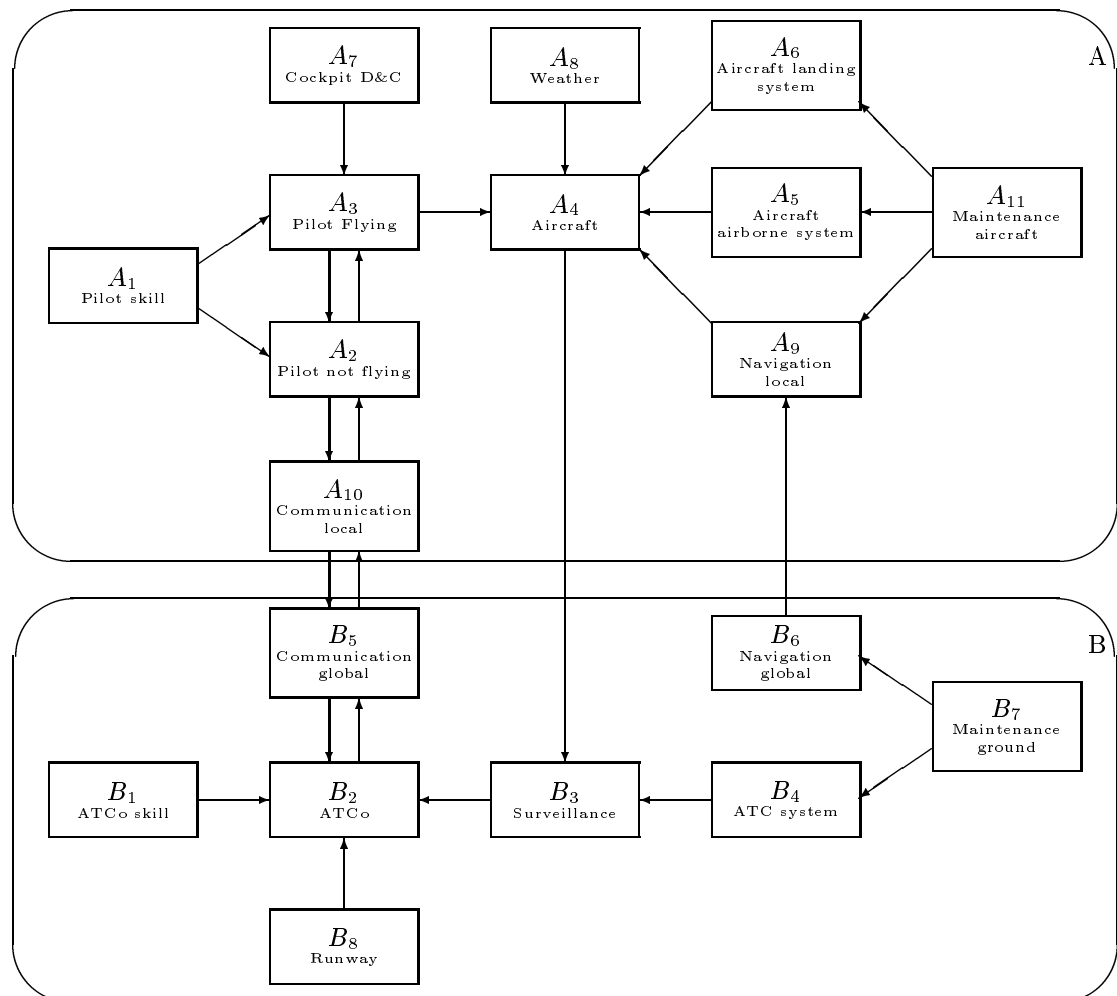


Figure 3 Functional representation of ATM.

For this particular risk assessment application it appeared to be sufficient to develop a Petri net for the aircraft behaviour only. One such Petri net is necessary for each aircraft separately. This Petri net is represented by the graph in Figure 4. This graph consists of four kinds of symbols: \circ = place ; \square = delaying transition ; $|$ = immediate transition and \rightarrow = arc. An arc either goes from a place to a transition or vice versa. In this Petri net, the places correspond to physical flight segments. The identified flight segments are determined by the following points: Outer

Marker (OM), Minimum Radar Vectoring Altitude (MRVA), Touchdown (TD), Missed Approach (MA) and Final MA Altitude (FMAA).

The dynamic status of the Petri net is shown through the appearance of one or more tokens in places and a dynamic colour value connected to each token. In a DCPN, a token colour value may evolve according to a (stochastic) differential equation, the characteristics of which depend on the place of the token. The solution of such differential equation may for example represent the aircraft state evolution.

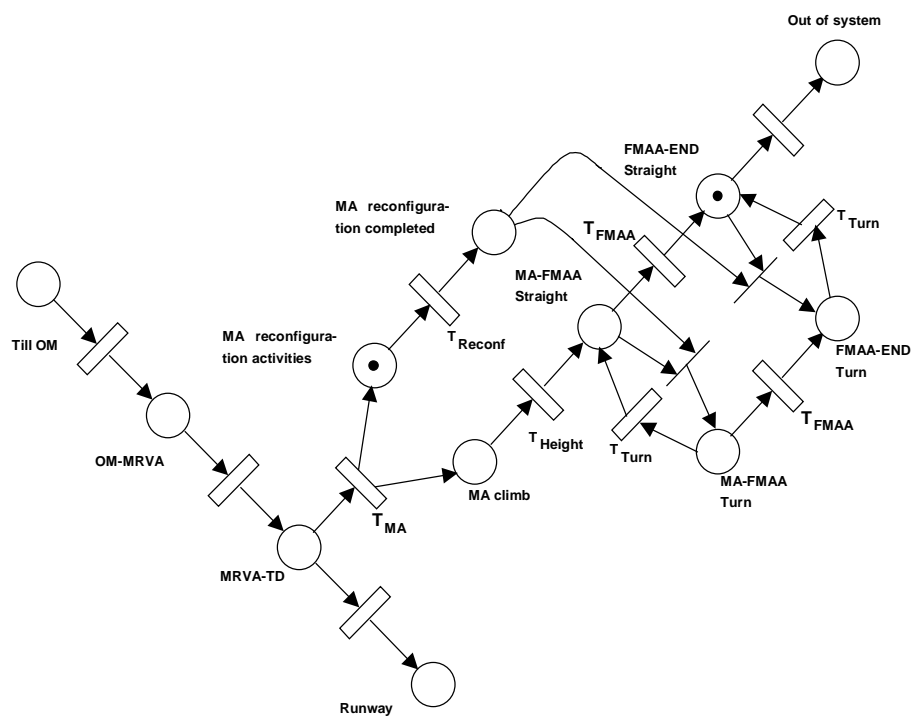


Figure 4 Aircraft state evolution Petri net: detailed level. Drawn is a feasible two-token situation, one token in place 'MA reconfiguration activities' and one token in place 'FMAA-END Straight'. Then the immediate transition to 'FMAA-END Turn' will fire as soon as the guard function of T_{Reconf} evaluates to true.

The Petri net in Figure 4 has two immediate transitions: 1) To MA-FMAA turn, and 2) To FMAA-END turn. These transitions are executed (fired) as soon as the transition is enabled (i.e. there is a token in each place from which there is an arc). All other transitions are guard transitions, which means that from the moment that the transition is enabled an additional condition has to become true prior to the actual firing of the transition. Table 6 specifies these guard transition delays.



On the basis of such a DCPN specification it is rather straightforward to make a software implementation to run Monte Carlo simulations. In theory, collision risk assessment is then a matter of running Monte Carlo simulations and then counting the events at which aircraft shapes physically start to overlap. In practice, this approach finds its limitation in the number of Monte Carlo simulations that can be reasonably run within a few hours³. In order to improve on this, stochastic analysis is used to decompose the collision risk in parts, each of which can be assessed separately. In order to take maximal advantage of the particular encounter situation under study and the statistical data available, the development of such a risk decomposition is situation specific. Below, we outline how this is done for the double MA scenario, following [Blom et al., 2001c].

Transition	Guard function evaluates to True if:
To OM-MRVA	Aircraft passes OM abeam
To MRVA-TD	Aircraft passes MRVA
To Out of system	Aircraft travelled 25km beyond threshold
T _{MA}	Aircraft reaches a randomly drawn altitude to start the MA.
T _{Height}	Pilot decides that aircraft has reached sufficient altitude to turn.
T _{Reconf}	Aircraft reconfiguration activities are completed
T _{Turn}	The prescribed or instructed turn is completed
T _{FMAA}	Aircraft reaches final MA altitude
To runway	Touch Down of aircraft

Table 6 Guard transitions in Figure 4.

3.2 Risk of collision between aircraft

Let $y_t^i := (y_{x,t}^i, y_{y,t}^i, y_{z,t}^i)$ and $v_t^i := (v_{x,t}^i, v_{y,t}^i, v_{z,t}^i)$ be the 3D location and 3D velocity of aircraft i ; the subscripts x and y refer to the axis system in Figure 1, and subscript z stands for the height. Let $y_t^{ij} := y_t^i - y_t^j$ be the distance between aircraft i approaching runway 19R and aircraft j approaching runway 22 at time t and let $v_t^{ij} := v_t^i - v_t^j$ be the relative velocity of aircraft i on runway 19R and aircraft j on runway 22 at time t .

Define D^{ij} as the collision area of $\{y_t^{ij}\}$, such that $y_t^{ij} \in D^{ij}$ means that at moment t the physical volumes of aircraft i and j are not separated anymore, i.e. they have collided. For aircraft encounters on final MA altitude, the collision area D^{ij} is a rectangular box, defined as $[-d_x^{ij}, d_x^{ij}] \times [-d_y^{ij}, d_y^{ij}] \times [-d_z^{ij}, d_z^{ij}]$, with $d_r^{ij} \equiv \frac{1}{2} d_r^i + \frac{1}{2} d_r^j$ and where the parameters d_x^i , d_y^i and d_z^i represent x , y and z -direction sizes of aircraft i respectively. For aircraft encounters during MA climb, the collision area D^{ij} depends on the inclination angle of the aircraft.

³ With one million Monte Carlo runs, the assessed collision frequency is significant to the level of 10^{-5} .



It is possible that the process $\{y_t^{ij}\}$ enters the area D^{ij} several times; each such occurrence is called an incrossing. Each occurrence of the process $\{y_t^{ij}\}$ leaving the area D^{ij} is called an outcrossing. The first incrossing for aircraft pair (i,j) on runways 19R and 22 is a collision for that pair. Hence, the incrossing rate is an upper bound for collision rate. ICAO collision risk models are accustomed to use this upper bound [Hsu, 1981].

Following reference [Bakker and Blom, 1993], the risk of collision R between two aircraft is expressed to be equal to a tight upper bound for the expected number of incrossings, between one aircraft i and another aircraft j in an appropriate time-interval $[0, T]$ as follows

$$R = \int_0^T \varphi^{ij}(t) dt \quad (1)$$

where $\varphi^{ij}(t)$ is the incrossing rate between aircraft i and j , which is defined as

$$\varphi^{ij}(t) \equiv \lim_{\Delta \downarrow 0} \frac{P(y_t^{ij} \notin D^{ij}, y_{t+\Delta}^{ij} \in D^{ij})}{\Delta} \quad (2)$$

From here on, in this paper time T is always chosen large enough such that the probability that the aircraft pair (i,j) collides outside interval $[0, T]$ is negligibly small.

3.3 Collision risk per approach

Now define R_Σ as the probability that aircraft i and j make MAs on 19R and 22 respectively, and both aircraft collide with each other. Also define *stopping times* τ^i and τ^{ij} for aircraft i and the pair (i, j) as

$$\tau^i \equiv \inf \{ T, t \mid \text{Aircraft } i \text{ initiates a MA at } t \}$$

and

$$\tau^{ij} \equiv \max \{ \tau^i, \tau^j \}.$$

From equation (1) and the definition of τ^{ij} it follows that R_Σ satisfies

$$R_\Sigma = \sum_j \int_{\tau^{ij}}^T \varphi^{ij}(t) dt \quad (3)$$

where the summation is over all runway 22 aircraft j .



3.4 Aircraft types and double missed approach causes

The event sequence classification process $\{\kappa_t^{ij}\}$ for an aircraft pair (i,j) consists of a local (i.e. aircraft) related process and a common related process. Here, this process is defined as $\kappa_t^{ij} \equiv \text{Col} \{ \kappa^i, \kappa^j, \kappa_t^G \}$, where κ^i and κ^j represent the aircraft types considered for aircraft i and j respectively, and where the process $\{ \kappa_t^G \}$, with $\kappa_t^G \in K^G$, represents the specific MA condition for both aircraft i and j . The set K^G represents a set of double MAs due to various reasons, i.e.

$$K^G \equiv \{ \text{Coinc, Tower, Wind, Alert, Meteo, Mixed} \}.$$

Now, we identify the value of $\{\kappa_t^{ij}\}$ at moment τ^{ij} as a relevant *event sequence class* $\kappa_{\tau^{ij}}^{ij}$.

Hence

$$\kappa_{\tau^{ij}}^{ij} \equiv \text{Col} \{ \kappa^i, \kappa^j, \kappa_{\tau^{ij}}^G \}.$$

Conditioning on event sequence class $\kappa_{\tau^{ij}}^{ij}$ and rearranging summation and integral yields

$$R_{\Sigma} = \sum_j \sum_{\kappa \in K} P \{ \kappa_{\tau^{ij}}^{ij} = \kappa \} \int_{\tau^{ij}}^T \varphi_{\kappa}^{ij}(t) dt \quad (4)$$

where set K is defined as $K \equiv K^i \otimes K^j \otimes K^G$ with K^i and K^j the sets of aircraft types of model assumption **M.20**, for aircraft i and aircraft j respectively. Moreover, $\varphi_{\kappa}^{ij}(t)$ is the $\kappa_{\tau^{ij}}^{ij}$ conditional incrossing rate between aircraft i and aircraft j , with aircraft i on one runway and aircraft j on the other runway, which is defined as

$$\varphi_{\kappa}^{ij}(t) \equiv \lim_{\Delta \downarrow 0} \frac{P(y_t^{ij} \notin D^{ij}, y_{t+\Delta}^{ij} \in D^{ij} \mid \kappa_{\tau^{ij}}^{ij} = \kappa)}{\Delta}$$

3.5 Decomposition over manoeuvre combinations

Through adopting some technical assumptions and a lengthy derivation it is possible to extend the risk decomposition of equation (4) to MA manoeuvre combinations and to identify what the summation over j means in terms of Monte Carlo simulations. The resulting set of equations is [Blom et al., 2001c]:

$$R_{\Sigma} = \sum_{\kappa^G \in K^G} R_{\kappa^G} \quad (5)$$

$$R_{\kappa^G} = \hat{\rho}_{\kappa^G} \sum_{w_{19R} \in W_{19R}} \sum_{w_{22} \in W_{22}} P_{\kappa^G}(w_{19R}) \cdot P_{\kappa^G}(w_{22}) \cdot \mu_{\kappa^G}(w_{19R}, w_{22}) \quad (6)$$

with W_z the set of possible MA paths for runway z , and p_{κ^G} and μ_{κ^G} satisfy

$$\begin{aligned}
 p_{\kappa^G}(w_{19R}) &= \alpha_{\kappa^G} && \text{if } w_{19R} = \text{straight \& 2000 ft} \\
 &= (1 - \alpha_{\kappa^G}) && \text{else} \\
 p_{\kappa^G}(w_{22}) &= \alpha_{AIP} && \text{if } w_{22} = \text{straight \& 2000 ft} \\
 &= (1 - \alpha_{AIP}) && \text{else} \\
 \mu_{\kappa^G}(w) &= 2 \cdot \sum_{\kappa^a \in K^i} \sum_{\kappa^b \in K^j} P\left\{ \left(\kappa_{\tau^{ij}}^i, \kappa_{\tau^{ij}}^j \right) = \left(\kappa^a, \kappa^b \right) \right\} \\
 &\quad \cdot I^{ij} \left(\left(\kappa^a, \kappa^b, \kappa^G \right), w \right), \quad w \in W_{19R} \times W_{22}
 \end{aligned} \tag{7}$$

$$I^{ij}(\kappa, w) \equiv \int_{\tau^{ij}}^T \varphi_{\kappa}^{ij}(t, w) dt$$

with j such that $(\tau^j - \tau^i)$ has a uniform distribution on $[-180s, 60s]$.

3.6 Decomposition of incrossing rate

Following [Bakker and Blom, 1993], the conditional incrossing rate satisfies

$$\begin{aligned}
 \varphi_{\kappa}^{ij}(t, w) &= \sum_{r=x,y,z} \int_{\underline{D}_r} \left\{ \int_0^{\infty} v_r^{ij} p_{y_r^{ij}, v_r^{ij} | \kappa_{\tau^{ij}}^{ij}} \left(\underline{y}_r^{ij}, -d_r^{ij}, v_r^{ij} | \kappa, w \right) dv_r^{ij} \right. \\
 &\quad \left. + \int_{-\infty}^0 -v_r^{ij} p_{y_r^{ij}, v_r^{ij} | \kappa_{\tau^{ij}}^{ij}} \left(\underline{y}_r^{ij}, d_r^{ij}, v_r^{ij} | \kappa, w \right) dv_r^{ij} \right\} d\underline{y}_r^{ij}
 \end{aligned} \tag{8}$$

where $p_{y_r^{ij}, v_r^{ij} | \kappa_{\tau^{ij}}^{ij}}(\cdot | \kappa, w)$ is the conditional probability density function for the aircraft relative position and velocity, \underline{D}_r is equal to collision area D^{ij} but without the r -th component, and \underline{y}_r^{ij} for $r = x, y, z$ is equal to the aircraft relative position without the r -th component.

Next, for an aircraft i and an aircraft j , *stopping times* τ_r^{ij} for $r=x,y,z$ are defined as follows

$$\tau_r^{ij} \equiv \inf \left\{ t \geq \tau^{ij} ; \left| y_{r,t}^{ij} \right| \leq d_r^{ij} \right\}$$

Together with (7) and (8) this implies



$$\begin{aligned}
 I^{ij}(\kappa, w) = & \sum_{r=x,y,z} \int_{\tau_r^{ij}}^T \int_{\underline{D}_r} \left\{ \int_0^{\infty} v_r^{ij} p_{y_r^{ij}, v_r^{ij}, t | \kappa^{ij}} \left(\underline{y}_r^{ij}, -d_r^{ij}, v_r^{ij} | \kappa, w \right) dv_r^{ij} \right. \\
 & \left. + \int_{-\infty}^0 -v_r^{ij} p_{y_r^{ij}, v_r^{ij}, t | \kappa^{ij}} \left(\underline{y}_r^{ij}, d_r^{ij}, v_r^{ij} | \kappa, w \right) dv_r^{ij} \right\} d \underline{y}_r^{ij} dt
 \end{aligned} \tag{9}$$

3.7 Numerical evaluation of equations

To assess risk numerically, first equation (9) is evaluated. For each relevant (κ, w) the following steps have to be performed:

- Monte Carlo simulation of double MAs on runways 19R×22.
- This yields histograms of simulated statistical information for the relative aircraft positions and speeds, to which sums of Gaussian densities are fitted.
- Equation (9) is solved through analytical integration over dv_r^{ij} and numerical integration over $d \underline{y}_r^{ij}$ and dt respectively.

Next, the numerical results for $I^{ij}(\kappa, w)$ are substituted into equation (7) and this into (6) and (5), to yield a numerical value for R_{Σ} .

This numerical evaluation scheme has to be performed for each of the operational scenarios that are presented next.



4 Risk assessment of operational scenarios

In this section, the risk assessment model is used to evaluate several SCIA operational scenarios for runway 19R×22. First, a series of operational scenarios is defined. Subsequently the risk assessment is performed in a sequence of steps. Finally, a comparison is made against established risk criteria.

4.1 Operational scenarios

The operational scenario variables identified for evaluation are:

- AIP published MA path for runway 19R: *Straight MA path* versus *Right Turn MA path*.
- Mixed mode operations, i.e. a departure in between two arrivals: *Allowed* versus *Not allowed*.
- Instructions by runway controller: *None* versus *Turn on 19R* versus *Extra climb on 19R*.

In total this yields 12 combinations, of which the ones in Table 7 are selected for risk assessment.

Operational scenario	19R MA in AIP	ATCo instruction	Mixed mode allowed
0	Straight MA on 19R	None	Yes
1	Straight MA on 19R	Turn on 19R	Yes
2	Straight MA on 19R	None	No
3	Straight MA on 19R	Turn on 19R	No
4	Straight MA on 19R	Extra climb on 19R	No
5	Turn MA on 19R	None	Yes
6	Turn MA on 19R	None	No

Table 7 Operational scenarios for risk assessment.

For each of these Operational scenarios in Table 7, the set of equations (5-9) has to be evaluated in a numerical sense. This is organised in two steps:

- Assess conditional collision risks $\mu_{k,G}(w)$ using equations (7,9)
- Assess collision risk $R_{k,G}$ and R_{Σ} using equations (5,6)

During subsequent third and fourth steps, bias and uncertainty in the risk values is assessed following [Everdij and Blom, 2002], and the bias and uncertainty corrected risk levels are compared against established risk criteria. The results of these four steps are given in the following four subsections.



4.2 Model based conditional collision risk

To evaluate equations (5) and (6) for the seven operational scenarios in Table 7, it appears that theoretically there is need to assess the conditional collision risk $\mu_{\kappa^G}(w)$ for $7 \times 6 \times 4 (=168)$ values of w . Practically, the effective number of w -values for which $\mu_{\kappa^G}(w)$ has to be evaluated is 12. These 12 combinations and the risk values $\mu_{\kappa^G}(w)$ assessed are given in Table 8.

w_{19R}	w_{22}	$\kappa^G \in \{\text{Tower, Wind}\}$	Other κ^G
Straight	Straight	$2.9 \cdot 10^{-3}$	$2.9 \cdot 10^{-3}$
Straight	Left turn	$3.7 \cdot 10^{-8}$	$2.4 \cdot 10^{-8}$
Right turn	Straight	$4.1 \cdot 10^{-8}$	$2.5 \cdot 10^{-8}$
Right turn	Left turn	$2.6 \cdot 10^{-8}$	$1.8 \cdot 10^{-8}$
Straight & Extra climb	Straight	$1.2 \cdot 10^{-5}$	$1.1 \cdot 10^{-5}$
Straight & Extra climb	Left turn	$< 3.7 \cdot 10^{-8}$	$< 2.4 \cdot 10^{-8}$

Table 8 Conditional collision risk values $\mu_{\kappa^G}(w)$ for the w -values that are relevant to assess the operational scenarios in Table 7.

To assess the conditional collision risks $\mu_{\kappa^G}(w)$ for each of the w -values in Table 8 according to equation (7), there appeared to be 120 (κ, w) combinations for which $I^{ij}(\kappa, w)$ needed to be numerically evaluated using (9).

As expected, all risk values of the Rayleigh PDF MA initiation height are higher than those for the Uniform PDF MA initiation height; the only exception is formed by the risk values for both aircraft making a straight MA. Also as expected is that the conditional collision risk values are worst when both aircraft make a straight MA. However, these risk values are almost five orders of magnitude worse than the risk values in case at least one of the aircraft makes a turn. The implication is that as long as there is a small chance that both aircraft make straight MAs then the conditional risk values at the top of Table 8 determine the total risk, and this is neutral regarding the precise shape of the MA initiation height PDF. This corresponds with the key finding of the phase 1 study [Blom et al., 2001b]. Another observation that can be made is that, for the runway combination considered, a turn appears to be more effective than an extra climb of 500 ft.

4.3 Model based collision risk

The next step in the assessment of collision risk is to evaluate equations (5) and (6) per scenario, using the conditional collision risk values from Table 8 and the $\hat{\rho}_{\kappa^G}$, α_{κ^G} and α_{AIP} values as these have been estimated in the section on modelling of missed approaches, taking into account the following specific sequence of adaptations:



- No Mixed Mode allowed means: $\hat{\rho}_{Mixed} = 0$
- Right turn MA on 19R in AIP means: replace α_{κ^G} by α_{AIP}
- No ATCo instruction means: replace α_{κ^G} by 1

The resulting collision risk values are presented in Table 9. This shows that the model-based total risks vary up to a factor of 100 with the scenario, with the Mixed Mode allowed scenario 0 having highest risk and scenarios 3, 4 and 6 having lowest risk. Before drawing further conclusions it is better to assess bias and uncertainty in these risk values first.

Scenario	0	1	2	3	4	5	6
R_{Coinc}	$4.5 \cdot 10^{-10}$	$6.7 \cdot 10^{-11}$	$4.5 \cdot 10^{-10}$	$6.7 \cdot 10^{-11}$	$6.9 \cdot 10^{-11}$	$4.5 \cdot 10^{-11}$	$4.5 \cdot 10^{-11}$
R_{Tower}	$2.9 \cdot 10^{-09}$	$1.5 \cdot 10^{-09}$	$2.9 \cdot 10^{-09}$	$1.5 \cdot 10^{-09}$	$1.5 \cdot 10^{-09}$	$2.9 \cdot 10^{-10}$	$2.9 \cdot 10^{-10}$
R_{Wind}	$5.1 \cdot 10^{-09}$	$7.6 \cdot 10^{-10}$	$5.1 \cdot 10^{-09}$	$7.6 \cdot 10^{-10}$	$7.8 \cdot 10^{-10}$	$5.1 \cdot 10^{-10}$	$5.1 \cdot 10^{-10}$
R_{Meteo}	$3.6 \cdot 10^{-09}$	$1.8 \cdot 10^{-10}$	$3.6 \cdot 10^{-09}$	$1.8 \cdot 10^{-10}$	$1.9 \cdot 10^{-10}$	$3.6 \cdot 10^{-10}$	$3.6 \cdot 10^{-10}$
R_{Alert}	$1.5 \cdot 10^{-09}$	$7.3 \cdot 10^{-11}$	$1.5 \cdot 10^{-09}$	$7.3 \cdot 10^{-11}$	$7.8 \cdot 10^{-11}$	$1.5 \cdot 10^{-10}$	$1.5 \cdot 10^{-10}$
R_{Mixed}	$1.2 \cdot 10^{-07}$	$5.8 \cdot 10^{-09}$	0	0	0	$1.2 \cdot 10^{-08}$	0
R_{Σ}	$1.3 \cdot 10^{-07}$	$8.3 \cdot 10^{-09}$	$1.3 \cdot 10^{-08}$	$2.5 \cdot 10^{-09}$	$2.6 \cdot 10^{-09}$	$1.3 \cdot 10^{-08}$	$1.4 \cdot 10^{-09}$

Table 9 Model based collision risks for SCIA on 19R×22.

Since the risk from double straight MAs provides the largest contributions, the values in Table 9 satisfy the following approximations:

$$\begin{aligned}
 R_{\kappa^G} &\approx \hat{\rho}_{\kappa^G} \cdot \alpha_{AIP} \cdot \mu_{\kappa^G} (Straight, Straight), \text{ scenarios 0, 2 and 6} \\
 &\approx \hat{\rho}_{\kappa^G} \cdot \alpha_{\kappa^G} \cdot \alpha_{AIP} \cdot \mu_{\kappa^G} (Straight, Straight), \text{ scenarios 1, 3 and 4} \\
 &\approx \hat{\rho}_{\kappa^G} \cdot \alpha_{AIP} \cdot \alpha_{AIP} \cdot \mu_{\kappa^G} (Straight, Straight), \text{ scenario 5}
 \end{aligned}$$

with

$$\hat{\rho}_{\kappa^G} \text{ values from Table 3 (with } \hat{\rho}_{Mixed} = 0 \text{ for scenarios 2, 3, 4, 6)}$$

$$\alpha_{\kappa^G} \text{ values from the first column in Table 5}$$

$$\alpha_{AIP} = 0.1 \text{ (model assumption M.29)}$$

$$\mu_{\kappa^G} (Straight, Straight) = 2.9 \cdot 10^{-3} \text{ (first row in Table 8)}$$



4.4 Bias and uncertainty assessment

The risk values in Table 9 apply to the mathematical model of the operational scenarios. Since such a mathematical model differs from reality, one should expect that the model-based risk differs from the true risk. The question then is to assess this difference in terms of bias and uncertainty relative to the model based risk. Recently, Everdij and Blom [2002] have developed a methodology to conservatively assess the bias and the 95% uncertainty band due to these differences. To apply this methodology to the SCIA scenarios of Table 9, we first give the equations of the total expected risk R_{Σ}^* :

$$R_{\Sigma}^* = B \cdot \exp\left\{\frac{1}{8} C\right\} \cdot R_{\Sigma} \quad (10)$$

with bias factor B and 95% uncertainty band (up and down) factor $\exp\sqrt{C}$ satisfying:

$$B = f_C^{(n_{CO}-n_{CP})} \cdot f_S^{(n_{SO}-n_{SP})} \cdot f_M^{(n_{MO}-n_{MP})} \cdot f_{Sm}^{(n_{SmO}-n_{SmP})} \cdot f_N^{(n_{NO}-n_{NP})} \quad (11)$$

$$C = n_{CU} \cdot (\ln f_C)^2 + n_{SU} \cdot (\ln f_S)^2 + n_{MU} \cdot (\ln f_M)^2 + n_{SmU} \cdot (\ln f_{Sm})^2 + n_{NU} \cdot (\ln f_N)^2 \quad (12)$$

where $n_{XY} \equiv$ total number of XY valued model assumptions, with $X \in \{\text{Considerable (C), Significant (S), Minor (M), Small (Sm), Negligible (N)}\}$, and with $Y \in \{\text{Pessimistic (P), Uncertain (U), Optimistic (O)}\}$, and with factors

$$\begin{aligned} f_C &= f_M^4 && \approx 5.06 \\ f_S &= f_M^2 && = 2.25 \\ f_M & && = 1.5 \\ f_{Sm} &= \sqrt{f_M} && \approx 1.2 \\ f_N &= \sqrt{f_{Sm}} && \approx 1.1 \end{aligned}$$

Here, pessimistic expected direction means that the modelled risk increases due to the assumption (i.e. the expected risk will be smaller than the model based risk). Optimistic expected direction means that the modelled risk reduces due to the assumption (i.e. the expected risk will be larger). Uncertainty expected direction means that it is expected that the influence on the modelled risk results is uncertain.

In this approach, positive and negative bias factors may (partly) compensate each other, while uncertainty band factors accumulate in a non-linear way. This approach requires safety conservative assessment of model assumptions against reality. Due to such safety conservatism



the chance that the risk falls above and below the assessed uncertainty band is 2.5% or less and 2.5% or more, respectively.

To assess the impact of all assumptions on collision risk and to determine uncertainty bands, all modelling assumptions except **M.15** (i.e. no TCAS) are assessed in a particular sequence to take into account dependencies [Everdij and Blom, 2002]. In case of lack of knowledge, a safety conservative approach has been taken. For parameter value assumptions the contribution to the uncertainty is assessed with support of model based parameter sensitivity analysis. The results of this assessment are presented in Table 10.

	0	1	2	3	4	5	6
SP	M.31	M.31	M.31	M.31	M.31	M.31	M.31
MP	-	-	-	-	-	-	-
SmP	-	-	-	-	-	-	-
NP	7×	7×	7×	7×	7×	7×	7×
CU	-	-	-	-	-	M.29	M.29
SU	M.29 M.30a	M.29 M.30a M.30b	M.29	M.29 M.30b	M.29 M.30b	M.30a	-
MU	M.6b	M.6b	M.6b M.30a	M.6b M.30a	M.6b M.30a	M.6b	M.6b M.30a
SmU	2×	3×	2×	3×	3×	2×	2×
NU	20×	20×	20×	20×	20×	20×	20×
SO	-	-	-	-	-	-	-
MO	-	-	-	-	-	-	-
SmO	-	-	-	-	-	-	-
NO	5×	5×	5×	5×	5×	5×	5×

Table 10 Overview of main results of expected effects of assumptions on the collision risk for the various scenarios. The model assumptions are introduced in the section on modelling. Model assumption M.15 (No TCAS) is not evaluated.

By counting the n_{XY} 's in Table 10 and substituting this in equations (10-12) we get the results in

Figure 5 and in the last row of Table 11. To complete Table 11, we use $R_{k^G}^* = R_{k^G} \cdot \frac{R_{\Sigma}^*}{R_{\Sigma}}$.



Runway combination 19R x 22

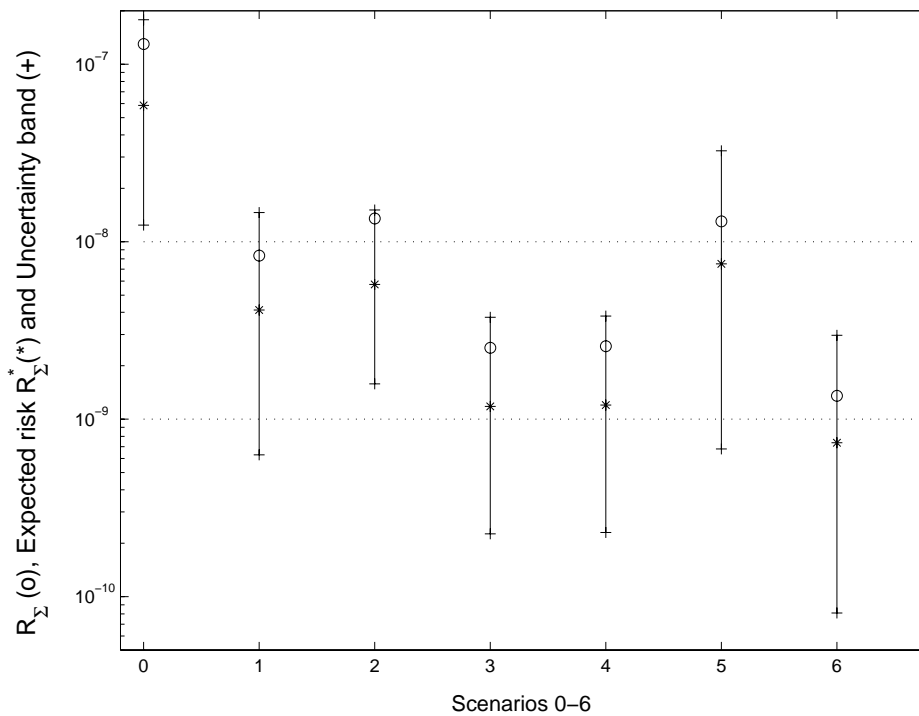


Figure 5 Model based risk $R_{\Sigma}(o)$, expected risk $R_{\Sigma}^*(*)$ and uncertainty band (++) , assuming No TCAS.

Scenario	0	1	2	3	4	5	6
R^*_{Coinc}	$2.0 \cdot 10^{-10}$	$3.3 \cdot 10^{-11}$	$1.9 \cdot 10^{-10}$	$3.1 \cdot 10^{-11}$	$3.2 \cdot 10^{-11}$	$2.6 \cdot 10^{-11}$	$2.4 \cdot 10^{-11}$
R^*_{Tower}	$1.3 \cdot 10^{-09}$	$7.2 \cdot 10^{-10}$	$1.2 \cdot 10^{-09}$	$6.7 \cdot 10^{-10}$	$6.8 \cdot 10^{-10}$	$1.7 \cdot 10^{-10}$	$1.6 \cdot 10^{-10}$
R^*_{Wind}	$2.3 \cdot 10^{-09}$	$3.8 \cdot 10^{-10}$	$2.2 \cdot 10^{-09}$	$3.5 \cdot 10^{-10}$	$3.6 \cdot 10^{-10}$	$2.9 \cdot 10^{-10}$	$2.8 \cdot 10^{-10}$
R^*_{Meteo}	$1.6 \cdot 10^{-09}$	$9.0 \cdot 10^{-11}$	$1.5 \cdot 10^{-09}$	$8.4 \cdot 10^{-11}$	$9.0 \cdot 10^{-11}$	$2.1 \cdot 10^{-10}$	$2.0 \cdot 10^{-10}$
R^*_{Alert}	$6.6 \cdot 10^{-10}$	$3.6 \cdot 10^{-11}$	$6.2 \cdot 10^{-10}$	$3.4 \cdot 10^{-11}$	$3.6 \cdot 10^{-11}$	$8.4 \cdot 10^{-11}$	$7.9 \cdot 10^{-11}$
R^*_{Mixed}	$5.3 \cdot 10^{-08}$	$2.9 \cdot 10^{-09}$	0	0	0	$6.7 \cdot 10^{-09}$	0
R^*_{Σ}	$5.9 \cdot 10^{-08}$	$4.1 \cdot 10^{-09}$	$5.7 \cdot 10^{-09}$	$1.2 \cdot 10^{-09}$	$1.2 \cdot 10^{-09}$	$7.5 \cdot 10^{-09}$	$7.4 \cdot 10^{-10}$

Table 11 Expected collision risk R_{Σ}^* for the scenarios, assuming No TCAS.

4.5 Comparison against risk criteria

For the SCIA operation considered, a generally accepted safety requirement does not exist. Nevertheless, relevant comparisons can be made: 1) a comparison with the maximal JAR allowable 10^{-9} of catastrophic risk per flying hour and per airborne system failure [JAR 25.1309], and 2) a comparison regarding an adequate use of SCIA to reduce the flight arrival delay, and thus also the collision risk exposure due to reduced flying time (e.g. in the stack).



JAR based criterion

If we assume that the average duration of a flight is two hours, then the maximal JAR allowable catastrophic risk per flight and per airborne system failure is $2 \cdot 10^{-9}$. If we were to adopt this same criterion for allowing catastrophic risk per external cause then most of the individual terms in Table 11 appear to satisfy this criterion. The exceptions are the Mixed mode terms in scenarios 0, 1 and 5, and the Wind terms in scenarios 0 and 2. It should be noticed that any possible effect of TCAS is not taken into account in the estimated risk values of Table 11.

ICAO based criterion

To gain further insight we express the expected extra risk in terms of the number of minutes extra flying time that would lead to a similar risk of collision with another aircraft. The rationale behind this is that the reason for conducting SCIA operations is to increase capacity in order to reduce delay (= extra flying time) in the order of minutes per arrival. This reduction in flying time itself implies a reduction in risk of collision with another aircraft (e.g. in the stack). To gain insight into this effect we assume that the exposure of collision with another aircraft corresponds with the TLS adopted by ICAO for fatal accidents per en-route flight hour without taking into account TCAS. Per direction (vertical, lateral, longitudinal) the TLS is $5 \cdot 10^{-9}$ fatal accidents per flight hour [ICAO, 1998], thus for three directions this is $1.5 \cdot 10^{-8}$ fatal accidents per flight hour. Expressing the expected collision risk values of Table 11 in terms of extra flying minutes with similar risk exposure this yields Table 12.

Scenario	0	1	2	3	4	5	6
Extra flying time	236 min.	17 min.	23 min.	5 min.	5 min.	30 min.	3 min.

Table 12 Extra flying time with similar risk exposure.

This shows, if SCIA operation also reduces the flying time per arrival by 5 minutes, then under operational scenarios 3, 4 and 6, the SCIA operation does not increase the total risk per arrival. Practically, this means that the risk levels assessed for double MAs during SCIA operation on runways 19R×22 do not compromise safety under the following scenarios:

- Scenario 3: Mixed mode is not allowed, AIP prescribes a left turning MA path for 22 and in case of a double MA the ATCo instructs a turn for aircraft on 19R.
- Scenario 4: Mixed mode is not allowed, AIP prescribes a left turning MA path for 22 and in case of a double MA the ATCo instructs an extra climb for aircraft on 19R.
- Scenario 6: Mixed mode is not allowed and AIP prescribes left turning and right turning MA paths for runways 22 and 19R respectively.



Mitigating measures

Although a series of operational scenarios have been assessed, there are several mitigating measure options which have not been considered in this study, e.g.

- Mitigating measures taken such that the occurrence of key hazards is significantly reduced. (*Tower down, severe Wind, and Meteo down, in particular.*)
- Training of situation-dependent handling by tower air traffic controllers.
- Increase training of pilots for non-straight MAs.

This means that the assessed risk values for conducting SCIA on 19R×22 can be further decreased if so desired.



5 Conclusions

The aim of the paper was to show that an accident risk modelling based evaluation of SCIA on safety has certain advantages over the geometric methods used so far. As an illustrative example, in this paper a risk assessment has been performed regarding simultaneous instrument approaches on converging runway combination 19R×22 at Schiphol. In line with the accident risk assessment methodology of [Blom et al., 2001a], the following activities have been performed in an iterative way:

1. Identify the specific MA scenarios to be assessed, and gather information about nominal and non-nominal behaviour of simultaneous MA by making use of information regarding pilot and ATCo interviews, statistical analysis of various data bases and MA flight simulations conducted by experienced pilots.
2. Develop a stochastic dynamical model of the operation, including a systematic specification of the additional assumptions adopted.
3. Perform Monte Carlo simulations and mathematical analysis techniques to assess the model-based accident risk for the MA scenarios identified.
4. Perform an assessment of the model assumptions and the impact each of these assumptions has on the accident risks for each MA scenario.
5. Compare the risk results obtained for SCIA operations on runways 19R×22 to JAR and ICAO established fatal accident risk criteria.

5.1 Conclusions regarding SCIA on 19R×22

Regarding SCIA on 19R×22 of Schiphol the main findings of the study are:

- The main contribution to the risk is coming from the non-negligible chance that, in case of a double MA, both aircraft fly straight MA paths.
- The highest risk levels occur when simultaneous converging runway operations would be conducted during mixed mode operations (a departure in between arrivals). Mixed mode operations induce significantly higher double MA rates during simultaneous operations on converging runways and therefore the extra risk is significantly higher (factor between 3 to 10) than under non mixed mode operations.
- If Mixed mode operations are not allowed, then the largest contributions to risk come from (other) common causes such as Tower R/T blocked, severe Wind, Meteo info down and airport great Alert. Per approach, the expected extra risk values (probability of collision) lie between $5.7 \cdot 10^{-9}$ and $7.4 \cdot 10^{-10}$ (any possible effect of TCAS is not taken into account). Both these highest and lowest values apply to operational scenarios that do not involve controller intervention.



The identified uncertainty band around the expected risk values extends from about a factor 6 up in risk to a factor 10 or more down in risk. These areas aim to cover 95% of all possibilities for the risk in a conservative way. As such, 2.5% or less may be above the upper bound of the uncertainty band, and 2.5% or more may be below the lower bound of the uncertainty band. The main model assumptions that cause this band are:

1. ATCo of runway 22 does not instruct a turning MA (assumption **M.31**)
2. Expert estimated $\alpha_{K.G}$ and α_{AIP} values for missing a turning MA (assumption **M.29**, **M.30b**)
3. Statistics and expert based estimates for double MA frequencies $\hat{\rho}$ (assumption **M.30a**).

Further investigations to improve the knowledge in these areas is valuable if one likes to reduce the bias and uncertainty band. However this would not impact the main findings above. The evaluation of the model assumptions also shows that the impact on the expected risk of TERPS+3 criteria regarding MA initiation points and diverging MA paths are far less important for allowing simultaneous landings on 19R×22 at Schiphol than success rates in realizing turning MA paths and common cause statistics are.

Under operational scenarios of excluding mixed mode operations three scenarios have been evaluated for which the level of catastrophic risk due to double MAs under SCIA on runways 19R and 22 appeared to be lower than the ICAO [1998] allowed risk of mid-air collision during five minutes en-route flying:

1. AIP prescribed right and left turning MA paths for runways 19R and 22 respectively (scenario 6)
2. AIP prescribed left turning MA path for runway 22, and if necessary, an ATC instructed right turning MA path for aircraft on runway 19R (scenario 3)
3. AIP prescribed left turning MA path for runway 22, and if necessary, an ATC instructed extra climb of 500ft for aircraft on runway 19R (scenario 4).

Theoretically the risk levels for these scenarios are similarly small as the reduction in risk exposure to other aircraft, e.g. due to leaving aircraft 5 minutes shorter in stack when conducting SCIA operations on 19R×22. In view of such marginal net differences in theoretical risk level, one might conclude that SCIA operation on 19R×22 under one of the above mentioned three conditions does not compromise safety.

5.2 General conclusions regarding SCIA

The SCIA risk modelling study has revealed a number of issues which have not been addressed in previous studies:

- Common cause double MAs appear far more frequently than coincidental double MAs.



- Some of these common causes reduce the performance of ATC in a negative way, and some the other way around.
- It has been shown that it is possible to conduct SCIA operations at risk levels that are in healthy balance with risk criteria established by JAR and ICAO.
- The TERPS+3 criteria on the placing of the MAPt's and the non-overlapping primary surfaces appear to have remarkably little impact on the safety of the SCIA operation. With the novel insight it seems worthwhile to study the development of appropriate mitigating measures which potentially contribute to the further development of SCIA operations.

For the specific Schiphol example a reasoning has been proposed to show that SCIA does not compromise safety; neither in relative nor in absolute terms under conditions that fall outside the current TERPS+3 criteria for SCIA operations. For airports with frequent low ceilings it would be valuable to relax these criteria through the adoption of the accident risk assessment methodology discussed in this paper. For an optimal reduction of SCIA criteria a dedicated collection of site specific statistical data on MAs and their reasons would be of great value. Since the FAA prescribes a systematic reporting by ATC of simultaneous MA events while conducting SCIA [FAA, 1993] one may expect that such valuable information is available. By using this in combination with a systematic accident risk assessment modelling approach, one might reasonably expect that the TERPS+3 criteria can be relaxed significantly on a site specific basis; this would allow bringing into account site specifics on MA practices, probabilities of missing MAs, and double MA frequencies.

Acknowledgement

The authors would like to thank the anonymous reviewers and the editor for their helpful comments and suggestions in improving the paper.



6 References

- AIP (2000), *Aeronautical Information Publication*, The Netherlands.
- Bakker, G.J. and Blom, H.A.P. (1993), "Air Traffic Collision risk modelling", *Proceedings of the 32nd IEEE Conference on Decision and Control*, pp. 1464-1469, San Antonio, TX, December.
- Blom, H.A.P., Bakker, G.J., Blanker, P.J.G., Daams, J., Everdij, M.H.C. and Klompstra, M.B. (2001a), "Accident risk assessment for advanced ATM", In: *Air Transportation Systems Engineering*, Eds: G.L. Donohue and A.G. Zellweger, Progress in Astronautics and Aeronautics, AIAA, pp. 463-480. Also as NLR Report TP-2001-642.
- Blom, H.A.P., Bakker, G.J., Klompstra, M.B. and Speijker, L.J.P. (2001b), *Risk Analysis of Simultaneous Missed Approaches on Runways 19R and 22, WP2: Modelling and evaluation of collision risk*, NLR Report CR-2000-697.
- Blom, H.A.P., Klompstra, M.B. and Bakker, G.J. (2001c), *Accident risk due to missed approaches on converging runways 19R×22 at Schiphol airport, Part 1: Accident risk assessment*, NLR Report CR-2001-536-PT1.
- Blom, H.A.P., Bakker, G.J. and Klompstra M.B. (2001d), *Accident risk due to missed approaches on converging runways 19R×22 at Schiphol airport, Part 2: Appendices*, NLR Report CR-2001-536-PT2.
- Everdij, M.H.C., Blom, H.A.P. and Klompstra, M.B. (1997), "Dynamically coloured Petri Nets for Air Traffic Management safety purposes", *Proceedings of the 8th IFAC Symposium on Transportation Systems*, Chania, Greece pp. 184-189. Also as NLR Report TP 97493 L.
- Everdij, M.H.C. and Blom, H.A.P. (2000), *Piecewise Deterministic Markov Processes represented by Dynamically Coloured Petri Nets*, NLR report TP-2000-428.
- Everdij, M.H.C. and Blom, H.A.P. (2002), *Designing EATMS inherently safe - Bias and uncertainty in accident risk assessment*, TOSCA-II WP4 Phase 2 Final report, NLR report CR-2002-137, April.
- FAA (1993), *Simultaneous Converging Instrument Approaches (SCIA)*, FAA Order 7110.98A, June 23rd.
- FAA (1998), *Simultaneous Converging ILS Approaches Aided by FMS LNAV Missed Approach*, FAA Order 8260.40.C7, December 31st.
- Hsu, D.A. (1981), *The evaluation of aircraft collision probabilities at intersecting air routes*, J. of Navigation, Vol.34 (1981), pp.78-102.
- ICAO-CRM (1980), *Manual on the use of the Collision Risk Model (CRM) for ILS operations*, 1st edition, ICAO-Doc-AN/9274.
- ICAO (1988), *Simultaneous Operations on parallel or near parallel Instrument Runways (SOIR)*, ICAO Circular 207-AN/126, Montreal, Canada.



- ICAO RGCSP (1988), *Review of the general concept of separation panel, 6th meeting*, Report Volume 2, ICAO.
- ICAO (1996), *Procedures for Air Navigation Services – Aircraft Operations (PANS-OPS), Volume I: Flight procedures; Volume II: Construction of visual and instrument flight procedures*, ICAO Doc 8168-OPS/611, 1996.
- ICAO (1998), *Annex 11 – Air Traffic Services*, 12th edition, incorporating amendments 1-38, Green pages, attachment B, paragraph 3.2.1, July. JAR 25.1309 (1994), *Joint Aviation Requirements JAR-25, Large Aeroplanes*, Change 14, 27 May 1994 & Amendment 25/96/1 of 9 April 1996, including AMJ 25-1309: System design and analysis Advisory Material Joint, Change 14.
- McCartor, G.R., Hasman, F., Jones, A., Yates, J. and Ladecky S. (1997), *Independent Converging FMS/LNAV Missed Approach Evaluation*, FAA report DOT-FAA-AFS-450-74, June.
- Newman, L.C., Swedish, W.J. and Shimi, T.N. (1981), *Requirements for instrument approaches to converging runways*, Report numbers MTR-81W230 and FAA-EM-82-4, MITRE, McLean, Virginia, September.
- Smith, A.P., Mundra, A.D., Barker, D.R. and Dorfman, G.A. (1992), *The Dependent Converging Instrument Approach procedure: an analysis of its safety and applicability*, Final report DOT/FAA/RD-93-006, MITRE, November.
- Weiss, W.E. (1986), *Proposed single criterion for IFR approaches to converging runways*, Report numbers MTR-86W17 and FAA-DL5-86-2, MITRE, McLean, Virginia, July.



Acronyms and abbreviations

AIP	Aeronautical Information Publication
ATC	Air Traffic Control
ATCo	Air Traffic Controller
ATM	Air Traffic Management
DCIA	Dependent Converging Instrument Approaches
DCPN	Dynamically Coloured Petri Net
DH	Decision Height
FMAA	Final MA Altitude
FMS	Flight Management System
ICAO	International Civil Aviation Organisation
ILS	Instrument Landing System
JAR	Joint Aviation Requirements
LNAV	Lateral Navigation
MA	Missed Approach
MAPt	Missed Approach Point
MRVA	Minimum Radar Vectoring Altitude
OM	Outer Marker
PDF	Probability Density Function
R/T	Radio/Telephony
SCIA	Simultaneous Converging Instrument Approaches
TCAS	Traffic Collision Avoidance System
TD	Touchdown
TERPS	Terminal Instrument Approaches
TLS	Target Level of Safety
TOPAZ	Traffic Organization and Perturbation AnalyZer
TWR/APP	Tower/Approach



Symbols

α_{AIP}	Probability that a pilot forgets to make a turn during the MA as prescribed in the AIP
α_{Alert}	Probability that the 19R controller is not successful in letting the aircraft on 19R make a right turn in case of a double MA due to great Alert
α_{Coinc}	Probability that the 19R controller is not successful in letting the aircraft on 19R make a right turn in case of a coincidentally double MA
α_{Meteo}	Probability that the 19R controller is not successful in letting the aircraft on 19R make a right turn in case of a double MA due to Meteo info down
α_{Mixed}	Probability that the 19R controller is not successful in letting the aircraft on 19R make a right turn in case of a double MA due to Mixed mode operation
α_{Tower}	Probability that the 19R controller is not successful in letting the aircraft on 19R make a right turn in case of a double MA due to Tower R/T blocked
α_{Wind}	Probability that the 19R controller is not successful in letting the aircraft on 19R make a right turn in case of a double MA due to severe Wind
α_{κ^G}	Probability that the 19R controller is not successful in letting the aircraft on 19R make a right turn in case of MA condition κ^G for both aircraft
B	Bias factor
$\exp\sqrt{C}$	95% uncertainty band (up and down) factor
d_x^i, d_y^i, d_z^i	Sizes of aircraft i in x , y and z -direction
$d_x^{ij}, d_y^{ij}, d_z^{ij}$	Mean values of the x , y and z -direction sizes of aircraft i and aircraft j
D^{ij}	Collision area of $\{y_t^{ij}\}$
\underline{D}_r	Collision area D^{ij} without the r -th component for $r = x, y, z$
f_X	Factor, with $X \in \{\text{Considerable (C), Significant (S), Minor (M), Small (Sm), Negligible (N)}\}$
i, j	Aircraft indices
$I^{ij}(\kappa, w)$	Help function of κ and w defined in equation (9)
$\phi^{ij}(t)$	Incrossing rate between aircraft i and j
$\phi_{\kappa}^{ij}(t, w)$	Conditional incrossing rate between aircraft i and aircraft j
K	Set of aircraft types for aircraft i and j and set of double MAs due to various reasons
K^G	Set of double MAs due to various reasons
K^i, K^j	Set of aircraft types for aircraft i and aircraft j
$\{\kappa_t^{ij}\}$	Event sequence classification process for an aircraft pair (i, j)
κ^i	Aircraft related process representing aircraft types considered for aircraft i
κ^G	Common related process representing specific MA condition for both aircraft



κ_t^G	Common related process representing specific MA condition for both aircraft at time t
$\mu_{\kappa^G}(w)$	Conditional collision risks
n_{XY}	Total number of XY valued model assumptions, with $X \in \{\text{Considerable (C), Significant (S), Minor (M), Small (Sm), Negligible (N)}\}$ $Y \in \{\text{Pessimistic (P), Uncertain (U), Optimistic (O)}\}$
$p_{\kappa^G}(w_{19R})$	Probability function of possible MA path for runway 19R
$p_{\kappa^G}(w_{22})$	Probability function of possible MA path for runway 22
$p_{y_i^{ij} v_{r,t}^{ij} \kappa_{ij}^{ij}}(\cdot \kappa, w)$	Conditional probability density function for the aircraft relative position and velocity
R	Collision risk between two aircraft
R_{κ^G}	Model based collision risk between two aircraft for specific MA condition κ^G
R_{Σ}	Total model based collision risk (= Probability that aircraft i makes a MA on 19R and collides with an aircraft making a MA on runway 22)
$R_{\kappa^G}^*$	Expected collision risk between two aircraft for specific MA condition κ^G
R_{Σ}^*	Total expected collision risk
$\hat{\rho}_{\text{Alert}}$	Estimated frequency for double MA due to great Alert
$\hat{\rho}_{\text{Coinc}}$	Estimated frequency for coincidentally double MA
$\hat{\rho}_{\text{Meteo}}$	Estimated frequency for double MA due to Meteo info down
$\hat{\rho}_{\text{Mixed}}$	Estimated frequency for double MA due to Mixed mode operation
$\hat{\rho}_{\text{Single}}$	Estimated frequency for single MA
$\hat{\rho}_{\text{Tower}}$	Estimated frequency for double MA due to Tower R/T blocked
$\hat{\rho}_{\text{Wind}}$	Estimated frequency for double MA due to severe Wind
$\hat{\rho}_{\kappa^G}$	Estimated frequency of MA condition κ^G for both aircraft
t	Time
T	End of time period
T_1	MA initiation moment (i.e. Task 1)
T_i	Moment at which task i starts for $i = 1, 2, \dots, 9$
T_{FMAA}	Transition at which aircraft reaches final Missed Approach altitude
T_{MA}	Transition at which aircraft reaches a randomly drawn altitude to start the MA.
T_{Height}	Transition at which pilot decides that aircraft has reached sufficient altitude to turn.
T_{Reconf}	Transition at which aircraft reconfiguration activities are completed
T_{Turn}	Transition at which the prescribed or instructed turn is completed
τ^i	Stopping time for aircraft i
τ^{ij}	Stopping time for aircraft pair (i, j)
τ_r^{ij}	Stopping time for aircraft pair (i, j)



v_t^i	3D Velocity of aircraft i approaching runway 19R
v_t^j	3D Velocity of aircraft j approaching runway 22
$v_{r,t}^i$	Velocity of aircraft i in r -direction for $r = x, y, z$
v_t^{ij}	Relative velocity of aircraft i on runway 19R and aircraft j on runway 22 at time t
$w = (w_{19R}, w_{22})$	MA paths on runways 19R and 22 respectively
W_{19R}	Set of two possible MA paths for runway 19R
W_{22}	Set of two possible MA paths for runway 22
x	Horizontal axis along the centerline of runway 19R, with origin at the threshold
y	Axis perpendicular to the centerline of runway 19R, in the direction of runway 22, with the origin at the threshold
y_t^i	3D Location of aircraft i approaching runway 19R
y_t^j	3D Location of aircraft j approaching runway 22
$y_{r,t}^i$	Location of aircraft i in r -direction for $r = x, y, z$
y_t^{ij}	Distance between aircraft i approaching runway 19R and aircraft j approaching runway 22 at time t
Υ_r^{ij}	Aircraft relative position without the r -th component for $r = x, y, z$
z	Height